

USING A MAGNETOHYDRODYNAMIC MODEL TO ANALYZE POT STABILITY IN ORDER TO IDENTIFY AN ABNORMAL OPERATING CONDITION

Jacques Antille, René von Kaenel,
Alcan Primary Metal Europe
Reduction Technology Services Europe
CH 3960 Sierre, Switzerland

Abstract

A numerical simulation model solves the magnetohydrodynamic equations for the real geometries and busbar arrangements of operating cells. This model predicts the natural frequencies of oscillation of the cell, which can be identified by analyzing anode currents.

The model calculates how an anode change affects the natural frequencies. Measurements were made for a simulated anode change (simply isolating the anode), and for a real change (where material was deliberately allowed to sink and freeze to the cathode). The predicted fluctuations of anode currents were in good agreement with those measured in both cases, the frequency spectrum of the anode current indicating the presence or absence of bottom crust. Thus, analyzing the variations in the anode currents during normal operation can help in identifying the reasons for abnormal operation.

Introduction

General

Often when a pot goes unstable the reason is not immediately obvious. The nature and seriousness of the instability can be conveniently analyzed by recording the fluctuations of the current in an anode rod and then performing a Fast Fourier Transformation (FFT) on the time-variant current values to obtain the natural frequencies and their amplitudes. It would be useful in monitoring the state of the pot and deciding on corrective action if a tool were available that could indicate the nature of the problem in relation to the pattern of these natural frequencies.

One of the commonly known causes of instability is changing an anode, especially when two anodes at the same corner are changed at the same time. If the change is made without due care and attention, cover material falling from the anode can sink and freeze to form a bottom crust over the surface of the cathode, and it is often observed that this aggravates the instability.

A “perfect” anode change (AC) can be simulated by insulating the pair of anodes from the anode beam so that the current they would normally carry is distributed among the other anodes in the pot. Then the anode current fluctuations can be analyzed with the FFT as before. The shift in the FFT pattern from this idealized case to the one where a bottom crust is allowed to form can then be used as an indicator for bottom crust. For the sake of brevity, the simulated AC will be referred to as the “clean” and the one forming bottom crust as the “dirty” AC.

It is however both tedious and time-consuming to make such a test, and it may reduce production; furthermore, a separate test would be needed for each kind of departure from ideal operation. If a numerical simulation model were able to predict accurately enough the change in FFT pattern, then it could be used in conjunction with the observed FFT of the anode current to diagnose problems in operation. It is the object of this paper to demonstrate the successful use of such a numerical simulation in predicting the change in FFT pattern from a “clean” to a “dirty” anode change.

Observations were made on a normally running pot at the ISAL smelter (Icelandic Aluminium Co. Ltd., Straumsvik, Iceland). The pots are arranged end-to-end, and the side of a pot facing the pots carrying current in the opposite direction is referred to as the “inside”, the other as the “outside” of the pot. In the plant a “dirty” AC was made by deliberately allowing material to fall into the bath, and after the pot had fully recovered eight hours later the same anode was insulated from the beam, making a “clean” change. The current distributions in the anodes and in the cathode collector bars were measured, as were the fluctuations in the current of the anode rod in which they were the strongest. The results of the respective numerical simulations were compared with the analysis of these observations.

Reference [1] describes the general nature of this kind of numerical simulation model. The model used here is a combined three-dimensional thermal and magnetohydrodynamic numerical simulation model, various aspects of which are described in references [2] through [8]. This model has found practical application hitherto in reducing anode consumption [9] and in designing hot changes to the external busbar configuration to increase the stability margin and thus allow stable operation at higher levels of current [10], [11]. The last two references concern among others the busbar changes made at the SØRAL smelter (Sør-Norge Aluminium A/S, Husnes, Norway), where the current in a set of test pots was successfully increased from 125 kA, the level at which the two lines were operating, to 140 kA.

It is worth mentioning in passing that all the pots in both lines have now (two years later) been retrofitted with the same busbar modification, and are now operating regularly at 150 kA with a current efficiency slightly higher than they had when running at 125 kA before retrofitting.

The Model

Reference [11] describes some important aspects of how the model predicts stability, particularly as regards the interaction of the vertical and horizontal components of the magnetic field with the current. The model determines among other things the velocity of liquid bath and metal, electric and magnetic fields, metal surface contour and ledge shape, and takes account of the following aspects:

- three dimensions
- the shape of both the ledge and the cell cavity
- the liquid bath around the anodes
- pressure fields in both bath and metal

The effect of the external magnetic field is crucial. A simple wire-bar representation is used for the busbar configuration at the ends of the line and for the adjacent potrooms. The current density field is calculated for the pot under investigation during normal operation, and this field is translated in space for the other pots in the line, and also rotated where necessary.

As Figure 1 shows, the pot immediately downstream of the one under consideration is modeled in detail in three dimensions (in the figure, the pot of interest is on the left, and the current flows from left to right).

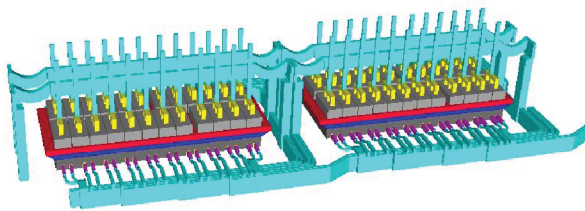


Figure 1: The 3D representation of the pot and its downstream neighbor

This is important because otherwise it would not be possible to determine the current distribution in the collector bars, which has a major effect on pot stability.

The metal surface contour is a free interface, which means that the pressure fields are calculated independently on both sides of it. The pressure at all points over the entire bath-metal interface must obviously be the same in bath and metal, so an iterative procedure is required. At each iteration, the complete model is run, i.e. a fresh calculation is made of the velocity, electric and magnetic fields, metal surface contour and ledge shape. The parameter ψ is the difference in pressure between bath and metal at the interface. The point on the interface is found where it is at a maximum and that at which it is at a minimum. Figure 2 gives typical values, the upper line showing the maxima and the lower line the minima. Ten iterations are typically required for the numerical simulation to converge.

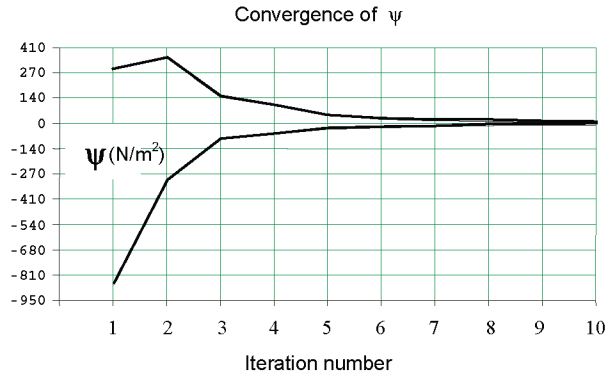


Figure 2 : Convergence of the numerical simulation model

Cell stability diagram

The model can be used to derive the stability diagram, which is a plot of the natural frequencies of oscillation in the complex plane, the eigenfrequencies. The real part, the frequency, is plotted on the x-axis, and the imaginary part, the stability criterion, on the y-axis. The stability diagram is described in more detail in [11]. Figure 3 is a typical stability diagram for the ISAL pot on which the measurements were made while it operated normally at 147 kA.

The broken line at -0.006 on the imaginary axis is the stability limit: if the plot of any individual eigenfrequency extends below this line, the pot is noisy and requires corrective action. The value -0.006 is not a theoretical one, but has been established by many observations of normal and more or less noisy pots in various smelters.

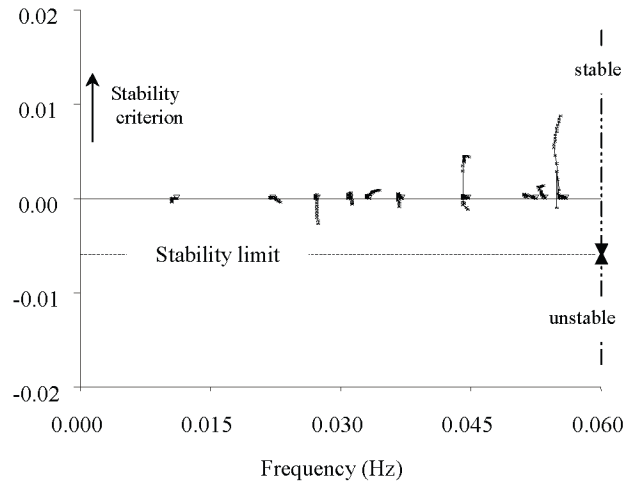


Figure 3: Stability diagram for a healthy pot at ISAL, operating at 147 kA

Results

The upper part of Figure 4 shows the measured collector bar current distribution for the outside of the pot as a percentage of the average current (the two upper traces), before and after the “ideal” anode change. The scale is on the left of the chart. The lower trace is the difference in share before and after the AC, with the scale on the right of the chart. The lower part of the figure gives the same information for the inside of the pot. The image of the anodes is superposed between the two charts, with the insulated anodes shaded. The four bars nearest to the insulated corner anode take a slightly smaller share of the current after the AC, on both sides of the pot; but the pattern of change is not significantly different from that for the other sixteen bars. The change in share ranges from +5% to -13%.

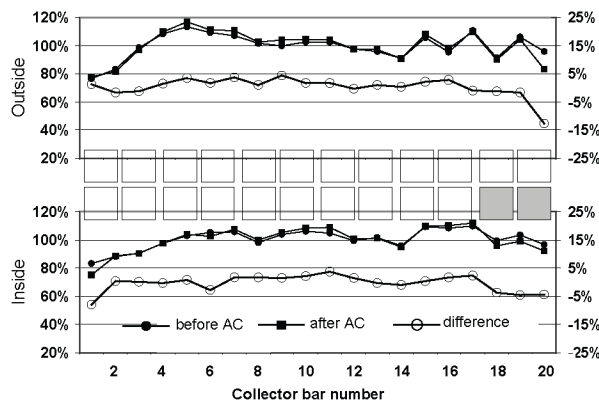


Figure 4 : Measured collector bar current distribution for the “clean” AC

The picture is very different after the real, “dirty” anode change (Figure 5).

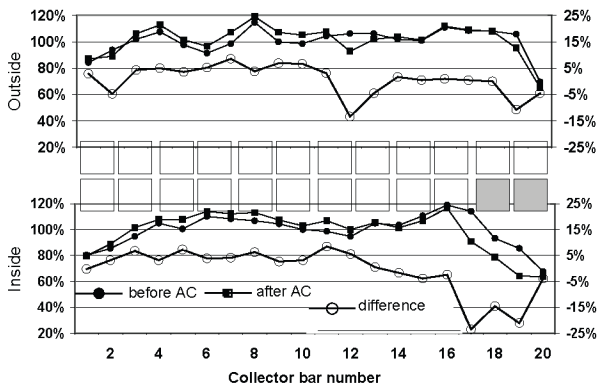


Figure 5 : Measured collector bar current distribution for the “dirty” AC

This disturbance in the collector bar current distribution is accompanied by considerable noise, as seen in Figure 6, which is a plot of the current variations in the rod of anode 23. This anode,

the one opposite to the changed anode, was chosen because it is the one showing the biggest oscillations and would thus give the clearest FFT trace. The current is oscillating $\pm 30\%$ about its mean value, with a period of about 28 seconds, or at about 0.036 Hz. The share of current taken by collector bars 17-20 on the inside, closest to the changed anodes, falls by about 16% and the pattern of the distribution is upset significantly on both sides of the pot. The change in share ranges from +11% to -25%.

In the numerical simulation, the cause of the “dirty” AC was represented as a layer of insulating material lying over the cathode immediately under the changed anode pair. Figure 7 shows the predicted collector bar current distributions after a “clean” AC, with a reasonably good variance, broadly in agreement with the corresponding traces in Figure 4. Figure 8 shows that after the AC with a partially insulated cathode. The variance has almost doubled, and again, the distributions agree broadly with those shown in Figure 5.

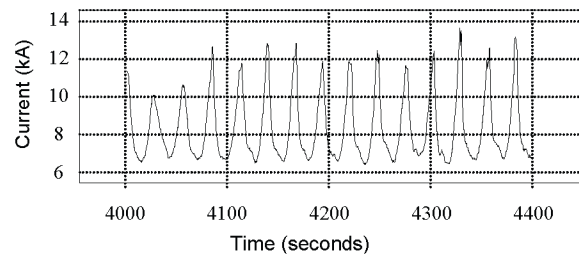


Figure 6: Fluctuation of current in anode rod 23

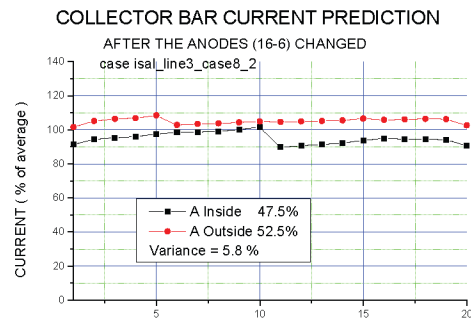


Figure 7 : Predicted collector bar current distribution after the “clean” AC

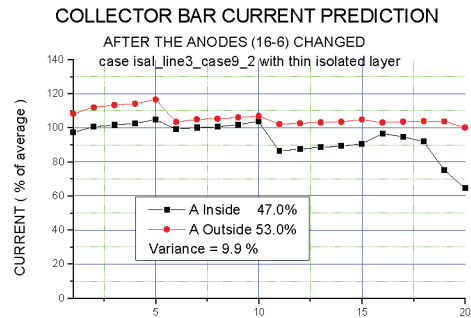


Figure 8 : Predicted collector bar current distribution after the “dirty” AC

Here the current share in collector bars 17-20 on the outside differs hardly at all from that after the “clean” change, but there is a drastic fall in the current share on the inside, bars 19 and 20 taking about 20-25% less than after the “clean” change. Thus the nature of the predicted change in collector bar current distributions agrees very well with that observed in practice.

Figure 9 shows the predicted velocity field at mid-height of the metal pad under normal operating conditions, and Figure 10 that after the “dirty” AC. The changed anode pair is located in the bottom right corner (shown shaded).

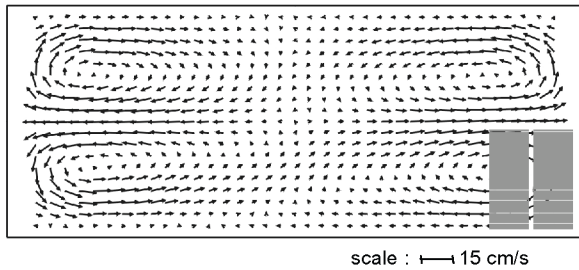


Figure 9: Velocity field under normal operation

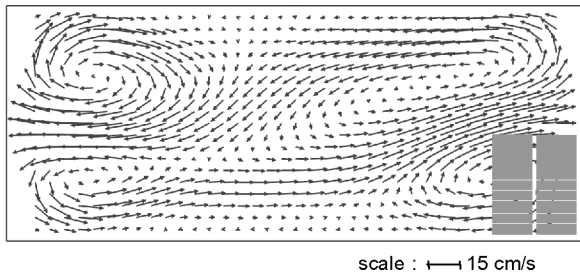


Figure 10: Velocity field after the “dirty” AC

The distortions in the pattern of velocity, and in particular the significant increase in velocity near the changed anodes, have a destabilizing effect.

Figure 11 illustrates the distortion of the current density in the metal under the corner anodes and just above the cathode block after the “clean” AC, and Figure 12 that after the “dirty” AC. The component of the density in the transverse direction is in fact significantly greater after the “clean” change than after the “dirty” one. Now by the simple stability criterion, which takes account only of the magnitudes of the field components, this would mean that the pot should be less stable after the “clean” than after the “dirty” AC. However, the gradients of the fields of current density (especially in the transverse direction) and of the magnetic field intensity (especially in the vertical direction) are bigger for the “dirty” than for the “clean” AC, and it is these gradients that are the real influences tending towards instability. The gradient of the current density field corresponds to the curvature of the current density streamlines in the figures, and one can see that those lines are much more tightly curved in Figure 12 than in

Figure 11. The model takes account in general of the interactions between the fields and between their Fourier components.

Figure 13 is the FFT corresponding to the measured anode rod current fluctuations after the “dirty” AC as already described (Figure 6). There is one dominant peak at 0.038 Hz. Figure 14 is the stability diagram from the corresponding numerical simulation, showing an eigenfrequency of 0.0388 Hz extending just beyond the stability limit.

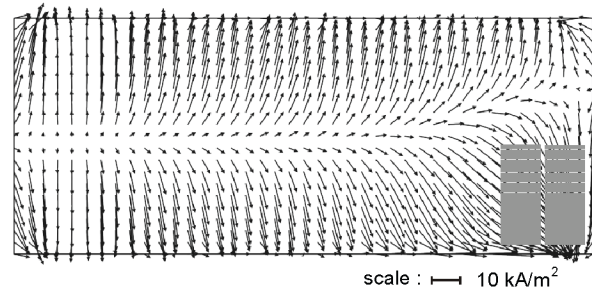


Figure 11 : Current density field after the “clean” AC

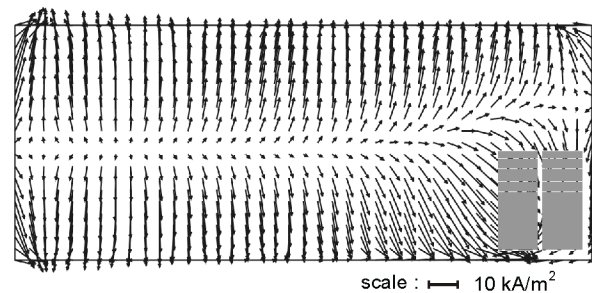


Figure 12: Current density field after the “dirty” AC

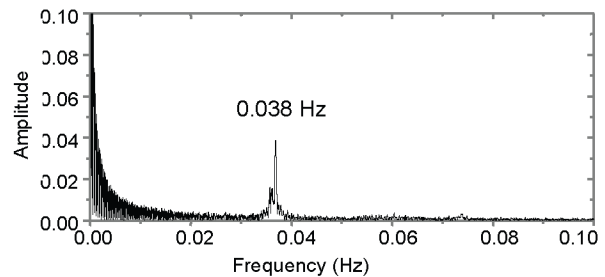


Figure 13: FFT of anode rod current fluctuations after the “dirty” AC

Considering that the model must predict the velocity and current density fields and the magnetic field as well as the ledge shape, and that all of these interact and have a big influence on the eigenfrequencies, the agreement with the both the FFT frequency of the anode current oscillation and the observed marginal stability of the pot is outstandingly good.

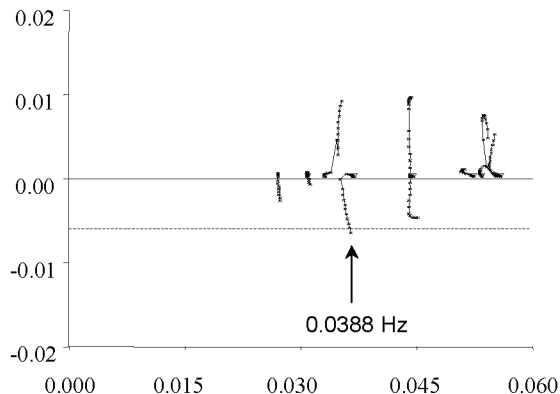


Figure 14 : Stability diagram after the “dirty” AC

The stability diagram for the “clean” AC, shown in Figure 15, shows a significant eigenfrequency at 0.044 Hz, but it is far from the stability limit.

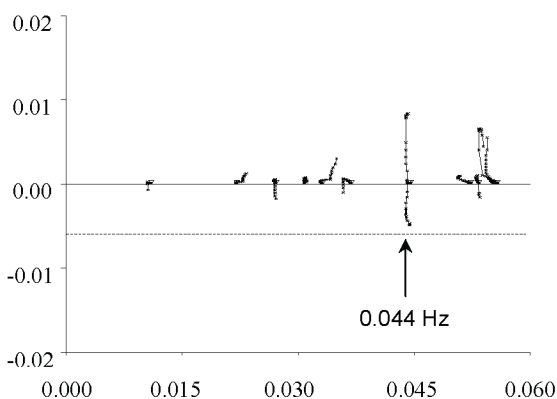


Figure 15 : Stability diagram after the “clean” AC

There is a very conspicuous difference between this and the dominant eigenfrequency for the “dirty” anode change.

Conclusions

1. The collector bar current distributions predicted by the numerical simulation model agree reasonably well with those observed, both for the “clean” and the “dirty” anode change. In particular, there is very good agreement with the change in distribution after the AC. The disturbed patterns of velocity and current density after the “dirty” AC indicate that the pot will be less stable.
2. The stability diagram for the “clean” AC indicates clearly that the pot will remain stable, the most significant eigenfrequency being 0.044 Hz.
3. The stability diagram for the “dirty” AC indicates equally clearly that the pot will be marginally stable, with one dominant eigenfrequency at 0.39 Hz, in remarkably close agreement with both the noisy state of the pot in practice and the

observed anode current oscillation at 0.038 Hz. This eigenfrequency is significantly different from the dominant frequency of the stable pot after the “clean” AC.

4. Thus the eigenfrequency spectrum described by the stability diagram in conjunction with an FFT analysis of the anode current fluctuations can give useful information about the operational state of the cathode.
5. It is reasonable to suppose that the same technique could be used successfully to identify other common difficulties in pot operation, such as inaccurate anode setting and anode spikes, among others. It should prove possible to obtain a sufficiently clear FFT picture from the pot voltage variations instead of the worst anode rod current variations that were used here. In that case, lines equipped with ALESA® pot controllers, which permit high frequency sampling of all the measured data over a suitable period, could be provided with automatic on-line diagnosis of such abnormal operating conditions.

Acknowledgements

The authors wish to express their thanks to the people at ISAL for their willing help with the measurements, and to Dr.Romerio and his team at the Swiss Federal Institute of Technology in Lausanne for their contributions to the modeling work.

References

- [1] M.Segatz, C.Droste, “Analysis of magnetohydrodynamic instabilities in aluminium reduction cells”, *Light Metals 1994*, pp 313-322, Ed. U.Mannweiler
- [2] R.von Kaenel, J.P.Antille, “On the stability of alumina reduction cells”, *Fifth Australasian aluminum smelter conference, 1995, Sydney, Australia*, Ed. B.Welch & M.Skyllas Kazacos, pp 530-544
- [3] J.Descloux, M.V.Romerio, M.Flück, *Linear stability of electrolysis cells Parts I,II, EPFL, DMA*, November 1990
- [4] J.Descloux, M.V.Romerio, M.Flück, *Stability analysis of an electrolysis cell for aluminium production by a perturbation method Parts I,II, EPFL, DMA*, September 1991
- [5] J.Descloux, M.Flück, M.V.Romerio, “Spectral aspects of an industrial problem”, *Spectral analysis of complex structure, Ed Hermann Paris, coordinator E.Sanchez Palencia 1995*, pp17-33
- [6] J.Descloux, M.Flück, M.V.Romerio, “Modeling for instabilities in Hall-Héroult cells: mathematical and numerical aspects”, *Magnetohydrodynamics in process metallurgy, Light Metals 1992*, Ed. by E.R.Cutshall, pp1195-1198
- [7] J.Descloux, Y.Jaccard, M.V.Romerio, *Stability in aluminium reduction cells: a spectral problem solved by an iterative procedure*, *Light Metals 1994*, pp 275-281, Ed. U.Mannweiler
- [8] J.Descloux, M.Flück, M.V.Romerio, “Modelling of the stability of aluminium electrolysis cell”, *Non-linear partial differential equations and their applications, College de France, Seminaire Volume XIII, Ed Longman 1998*, pp 117-133

- [9] J.P.Antille, P.Snaelund, J.M.Stefansson, R.von Kaenel, "Determination of metal surface contour and improved anode consumption", Light Metals 1997, pp 469-476
- [10] T.Johansen, H.P.Lange, R.von Kaenel, "Productivity increase at SØRAL smelter", Light Metals 1999, pp 153-157
- [11] J.P.Antille, R.von Kaenel, "Busbar optimisation using cell stability criteria and its impact on cell performance", Light Metals 1999, pp 165-170